Acta Cryst. (1997). B53, 708–718

A Study of Diastereomeric Mandelate Salts of Cinchonidine and the Relation to Their Quasidiastereomeric Analogues

ANNE GJERLØV AND SINE LARSEN*

Centre for Crystallographic Studies,† Department of Chemistry, University of Copenhagen, Universitetsparken 5, DK-2100 Copenhagen, Denmark. E-mail: sine@xray.ki.ku.dk

(Received 28 October 1996; accepted 3 March 1997)

Abstract

The crystal structures have been determined for the diastereomeric salts formed by cinchonidine and the two enantiomers of mandelic acid using low-temperature [122 (1) K] X-ray diffraction data. The less soluble salt is cinchonidinium (*S*)-mandelate, $C_{19}H_{23}N_2O^+.C_8H_7O_3^-$, M_r = 446.53, monoclinic, *C*2, a = 21.400 (2), b = 6.2777 (6), c = 17.853 (2) Å, β = 109.304 (8)°, V = 2263.6 (4) Å^3, Z = 4, D_x = 1.310 g cm^{-3}, λ(Cu $K\alpha$) = 1.54184 Å, μ = 7.08 cm^{-1}, F(000) = 952, R_1 = 0.0259 for 2684 observed reflections. The cinchonidine salt with (*R*)-mandelic acid, $C_{19}H_{23}N_2O^+.C_8H_7O_3^-$, has M_r = 446.53, monoclinic, $P2_1$, a = 6.410 (3), b = 32.808 (11), c = 11.222 (2) Å, β = 100.67 (2)°, V = 2319.2 (13) Å^3, Z = 4, D_x = 1.279 g cm^{-3}, λ(Cu $K\alpha$) = 1.54184 Å, μ = 6.91 cm^{-1}, F(000) = 952, R_1 = 0.0380 for 8951 observed reflections. The two salts have virtually identical hydrogen-bond patterns and similar herringbone stacking of the quinoline ring systems. The crystal packing of the two salts differ only with respect to the packing of the phenyl groups. The packing of the cinchonidinium mandelates is significantly different from the crystal packing in the corresponding mandelates of cinchonine. The lack of a quasidiastereomeric relationship between the two sets of salts can be attributed to the steric effects of the vinyl group. The similarities between the two cinchonidinium mandelate structures is a possible explanation to the similar solubilities of the salts. DSC and NMR measurements showed that the cinchonidinium salts undergo a chemical opening reaction in the solid state. The arrangement of hydrogen-bonded chains of alternating cations and anions appear to be important for the solid-state reaction to take place.

1. Introduction

Since Pasteur (1853) used a cinchona alkaloid to separate racemic tartaric acid into its enantiomers through the formation of diastereomeric salts, this method has been widely used to isolate enantiomers from a racemic mixture. Considering the applicability of this resolution process it is surprising that relatively little insight has been attained with respect to the structural and physicochemical basis for the difference in solubilities of the diastereomeric salts, which enables the separation of the enantiomers.

The cinchona alkaloids are frequently used for the resolution of racemic acids.

McKenzie (1899) had already studied the resolution of racemic mandelic acid with several cinchona alkaloids. He succeeded in isolating the two diastereomeric salts that could be formed with a given base and measured the solubilities for the less and more soluble diastereomeric salts. An efficient resolution relies heavily on the difference in the solubilities of the diastereomeric salts. Quinine gave the best resolution of mandelic acid, whereas cinchonidine was the least effective of the investigated resolving agents and McKenzie suggested that this may partly be attributed to the isomorphism of its salts. We have investigated the two structures and compared them with the structures of the two diastereomeric mandelate salts of cinchonine, which is a better resolving agent than cinchonidine. In our studies of the origin of the chiral discrimination responsible for the difference in solubilities of equivalent diastereomeric salts, we find that it is also important to include systems where the separation is less efficient in order to gain more information on the factors which determine the effectiveness of a compound to be used for this purpose.

The closely related cinchona alkaloids differ with respect to their stereochemistry and the substituents.

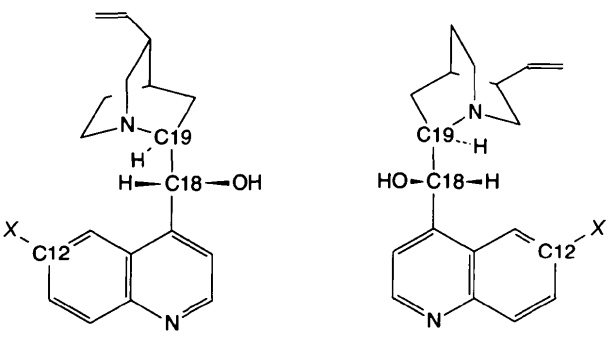

The Cinchona alkaloids.

Quinine, X = OCH$_3$ — Quinidine, X = OCH$_3$

Cinchonidine, X = H — Cinchonine, X = H

† Centre for Crystallographic Studies is funded by the Danish National Research Foundation.

The schematic drawings illustrate the stereochemical relationship between cinchonine and cinchonidine. The vinyl group creates two centres of chirality, apart from this the two bases are mirror images as they have opposite chiralities of C18 and C19. Therefore, it could be expected that they would form quasidiastereomeric salts, *e.g.* the (*R*)-mandelate salt of cinchonine would be similar to the (*S*)-mandelate salt of cinchonidine and *vice versa*. The structure determinations of the mandelate salts of cinchonidine have enabled us to compare diastereomeric salts with similar solubilities and study their relation to the structures of their quasidiastereomeric analogues the mandelates of cinchonine, which have been determined previously by Larsen, Lopez de Diego & Kozma (1993).

An interesting aspect of the cinchonidinium mandelates that emerged as part of their physico-chemical characterization is their ability to undergo a ring-opening reaction in the crystalline state. We have investigated this reaction further and believe that the specific hydrogen-bonding pattern in these salts is important for the reaction to take place.

2. Experimental

2.1. *Preparation of the cinchonidinium mandelates*

All compounds were prepared from analytical-grade chemicals purchased from Aldrich. Cinchonidinium (*S*)-mandelate was prepared from the pure acid and base: 1.4715 g (5.0 mmol) of cinchonidine and 0.7624 g (5.0 mmol) of (*S*)-mandelic acid were dissolved in 50 ml of methanol and left at room temperature. The crystals, which precipitated within a few days, were large and needle-shaped elongated along the crystallographic *b* axis. The equivalent (*R*) salt, cinchonidinium (*R*)-mandelate, was prepared by dissolving 0.7604 g (5.0 mmol) of (*R*)-mandelic acid in 35 ml of ethanol and neutralizing the solution with 1.4726 g (5.0 mmol) of cinchonidine. The solution was heated until all the base was dissolved and it was covered with parafilm with small holes for slow evaporation and cooling to room temperature. After 2 weeks the crystals formed were removed from the remaining ethanol and dried. The crystals are long thin needles growing into rosettes, elongated along the crystallographic *a* axis.

2.2. *Optical resolution of mandelic acid*

Racemic mandelic acid was resolved by cinchonidine. Racemic mandelic acid (0.7628 g, 5.0 mmol) was dissolved in 40 ml of water and neutralized by slowly adding 1.4708 g (5.0 mmol) of cinchonidine. The crystalline precipitate which formed quickly was isolated by filtration.

A Guinier–Hägg camera was used to record the powder diagrams of the cinchonidinium mandelates prepared from the pure enantiomers of mandelic acid and of this first precipitate from the resolution experiment at ambient temperature. Graphite-monochromated Cu $K\alpha$ radiation was used and Si employed as the internal standard. The powder pattern of the precipitate from the resolution with cinchonidine, which is formed within a few hours, corresponds to the powder pattern of the (*S*) salt.

2.3. *Thermoanalytical measurements*

Melting points were measured by differential scanning calorimetry using a Polymer Laboratories PL-DSC instrument calibrated with indium and tin. The measurements were carried out on powdered samples in closed crucibles. The heating rate was 5 K min^{-1} and sampling was made every 1.25 s. Thermogravimetric measurements showed that the salts retain more than 95% of their weight up to 493 K, which was the upper heating limit. DSC measurements were performed for the salts made from the pure acids and bases, for the first precipitate from the resolution experiment and for pure cinchonidine. The masses of the samples were between 3.6 and 5.4 mg, measured with a precision of 0.001 mg. Reheating experiments were carried out for the salts from the pure compounds and for pure cinchonidine.

2.4. *NMR spectroscopy*

^{13}C NMR spectra were measured for the salts from the pure compounds, as well as for samples that had been heated once. The salts were dissolved in $CDCl_3$. The measurements were performed with a Varian Unity 400 spectrometer at room temperature.

2.5. *X-ray crystallography*

Low-temperature X-ray intensity data were collected for both diastereomeric salts using a CAD-4 diffractometer. Cu $K\alpha$ (λ = 1.54184 Å) radiation was used, which was obtained from a graphite monochromator. The crystals were cooled with an Enraf–Nonius gas-flow low-temperature device and kept at 122 K during the experiment. The temperature was monitored with a thermocouple in the exhaust pipe; it remained constant within 1 K. Only a partial set of Friedel-related reflections were collected for the (*S*)-mandelate salt. Hence, the ratio of refined reflections to parameters is as low as 6.96 for this compound, whereas it is 11.81 for the (*R*)-mandelate salt, but the resulting structures appear to have both been determined with approximately the same precision. The orientation of the crystals was checked after every 600 reflections. The intensities of three standard reflections were measured every 10 000 s for each salt. The intensity decay was 4.2% for the (*S*)

Table 1. *Experimental details*

	(*S*)-Mandelate	(*R*)-Mandelate
Crystal data		
Chemical formula	$C_{19}H_{23}N_2O^+.C_8H_7O_3^-$	$C_{19}H_{23}N_2O^+.C_8H_7O_3^-$
Chemical formula weight	446.53	446.53
Cell setting	Monoclinic	Monoclinic
Space group	*C*2	$P2_1$
a (Å)	21.400 (2)	6.410 (3)
b (Å)	6.2777 (6)	32.808 (11)
c (Å)	17.853 (2)	11.222 (2)
β (°)	109.304 (8)	100.67 (2)
V (Å^3)	2263.6 (4)	2319.2 (13)
Z	4	4
D_x (Mg m^{-3})	1.310	1.279
Radiation type	Cu $K\alpha$	Cu $K\alpha$
Wavelength (Å)	1.54184	1.54184
No. of reflections for cell parameters	22	18
θ range (°)	37.91–45.19	16.23–30.18
μ (mm^{-1})	0.708	0.691
Temperature (K)	122 (1)	122 (1)
Crystal form	Needle	Needle
Crystal size (mm)	0.40 × 0.13 × 0.13	0.50 × 0.25 × 0.03
Crystal colour	White	White
Data collection		
Diffractometer	Enraf–Nonius CAD-4	Enraf–Nonius CAD-4
Data collection method	ω–2θ scans	ω–2θ scans
Absorption correction	None	Integration by crystal shape
T_{min}	–	0.833
T_{max}	–	0.991
No. of measured reflections	3022	10 960
No. of independent reflections	2707	9154
No. of observed reflections	2684	8951
Criterion for observed reflections	$I > 2\sigma(I)$	$I > 2\sigma(I)$
R_{int}	0.0124	0.0183
θ_{max} (°)	74.94	75.03
Range of *h*, *k*, *l*	$-26 \rightarrow h \rightarrow 25$	$-8 \rightarrow h \rightarrow 7$
	$-7 \rightarrow k \rightarrow 7$	$-40 \rightarrow k \rightarrow 40$
	$0 \rightarrow l \rightarrow 22$	$0 \rightarrow l \rightarrow 14$
No. of standard reflections	3	3
Frequency of standard reflections (min)	166.7	166.7
Intensity decay (%)	4.2	7.7
Refinement		
Refinement on	F^2	F^2
$R[F^2 > 2\sigma(F^2)]$	0.0259	0.0380
$wR(F^2)$	0.0723	0.1007
S	0.944	1.029
No. of reflections used in refinement	2707	9153
No. of parameters used	389	775
H-atom treatment	Only coordinates of H atoms refined	Only coordinates of H atoms refined
Weighting scheme	$w = 1/[\sigma^2(F_o^2) + (0.0583P)^2 + 0.7316P]$, where $P = (F_o^2 + 2F_c^2)/3$	$w = 1/[\sigma^2(F_o^2) + (0.0761P)^2 + 0.2265P]$, where $P = (F_o^2 + 2F_c^2)/3$
$(\Delta/\sigma)_{max}$	0.030	0.005
$\Delta\rho_{max}$ (e Å^{-3})	0.236	0.156
$\Delta\rho_{min}$ (e Å^{-3})	−0.201	−0.243
Extinction method	*SHELXL*93 (Sheldrick, 1994)	None
Extinction coefficient	0.0034 (2)	–
Source of atomic scattering factors	*International Tables for Crystallography* (Vol. C)	*International Tables for Crystallography* (Vol. C)
Absolute configuration	−0.01 (15) (Flack, 1983)	−0.06 (10) (Flack, 1983)
Computer programs		
Data collection	*CAD*-4 (Enraf–Nonius, 1989)	*CAD*-4 (Enraf–Nonius, 1989)
Cell refinement	*CAD*-4 (Enraf–Nonius, 1989)	*CAD*-4 (Enraf–Nonius, 1989)
Data reduction	*DREADD* (Blessing, 1987)	*DREADD* (Blessing, 1987)
Structure solution	*SHELXS*86 (Sheldrick, 1990)	*SHELXS*86 (Sheldrick, 1990)
Structure refinement	*SHELXL*93 (Sheldrick, 1995)	*SHELXL*93 (Sheldrick, 1995)
Preparation of material for publication	*SHELXL*93 (Sheldrick, 1995) and local programs	*SHELXL*93 (Sheldrick, 1995) and local programs

salt and 7.7% for the (*R*) salt. Additional details on the data collections are given in Table 1.

Data reduction was performed using the *DREADD* data reduction package (Blessing, 1987). Corrections were made for Lorentz, polarization and background effects and intensity decay. The crystal used for the data collection of the (*R*) salt was of a size and shape that made it necessary to correct the data for absorp-

Table 2. *Fractional atomic coordinates and equivalent isotropic displacement parameters (Å²) for (S)-mandelate*

$U_{eq} = (1/3)\Sigma_i\Sigma_j U^{ij} a_i^* a_j^* \mathbf{a}_i.\mathbf{a}_j$.

	x	y	z	U_{eq}
O1	0.37609 (6)	1.3514 (2)	0.40559 (6)	0.0264 (3)
O2	0.35692 (5)	1.0085 (2)	0.37234 (6)	0.0263 (2)
O3	0.44683 (7)	1.2764 (3)	0.55187 (7)	0.0417 (4)
C1	0.37937 (7)	1.1570 (3)	0.42122 (8)	0.0199 (3)
C2	0.41498 (7)	1.0954 (3)	0.50852 (8)	0.0237 (3)
C3	0.36863 (6)	0.9917 (3)	0.54614 (8)	0.0199 (3)
C4	0.34460 (8)	0.7867 (3)	0.52392 (9)	0.0271 (3)
C5	0.30254 (8)	0.6903 (3)	0.55873 (11)	0.0391 (5)
C6	0.28475 (8)	0.7958 (4)	0.61612 (11)	0.0424 (5)
C7	0.30795 (8)	0.9998 (4)	0.63839 (10)	0.0399 (5)
C8	0.35007 (7)	1.0984 (3)	0.60372 (9)	0.0270 (3)
O4	0.34996 (5)	0.3972 (2)	0.24814 (6)	0.0211 (2)
N1	0.16702 (6)	0.6252 (2)	0.00352 (7)	0.0248 (3)
N2	0.42981 (5)	0.8283 (2)	0.29556 (6)	0.0166 (2)
C9	0.26825 (6)	0.6129 (2)	0.15347 (7)	0.0178 (3)
C10	0.22121 (7)	0.7829 (3)	0.13545 (8)	0.0190 (3)
C11	0.22069 (7)	0.9505 (3)	0.18842 (8)	0.0234 (3)
C12	0.17379 (8)	1.1084 (3)	0.16643 (10)	0.0282 (3)
C13	0.12546 (8)	1.1082 (3)	0.08964 (10)	0.0297 (4)
C14	0.12464 (7)	0.9492 (3)	0.03761 (9)	0.0268 (3)
C15	0.17143 (7)	0.7817 (3)	0.05865 (8)	0.0220 (3)
C16	0.21079 (7)	0.4705 (3)	0.02383 (8)	0.0239 (3)
C17	0.26246 (7)	0.4573 (3)	0.09778 (8)	0.0204 (3)
C18	0.32665 (6)	0.6086 (2)	0.23064 (7)	0.0165 (3)
C19	0.38018 (6)	0.7558 (2)	0.21802 (7)	0.0159 (3)
C20	0.41851 (7)	0.6586 (3)	0.16698 (8)	0.0187 (3)
C21	0.49293 (7)	0.6996 (2)	0.20660 (8)	0.0182 (3)
C22	0.51708 (7)	0.5817 (3)	0.28603 (9)	0.0225 (3)
C23	0.47736 (7)	0.6568 (3)	0.33856 (8)	0.0201 (3)
C24	0.46784 (7)	1.0124 (2)	0.27826 (8)	0.0196 (3)
C25	0.50637 (7)	0.9388 (2)	0.22340 (8)	0.0183 (3)
C26	0.48947 (8)	1.0690 (3)	0.14861 (8)	0.0244 (3)
C27	0.53352 (10)	1.1677 (4)	0.12476 (12)	0.0422 (4)

tion effects using the Gaussian numerical integration procedure; the transmission factors were in the range 0.833–0.991. Reflections related by the symmetry of the crystal class were averaged. The structures were solved by direct methods using *SHELXS*86 (Sheldrick, 1990) and refined against F^2 using *SHELXL*93 (Sheldrick, 1993), minimizing $\Sigma_H w_H(|F_{HO}|^2 - |F_{HC}|^2)^2$ summed over all reflections. After anisotropic displacement parameters had been introduced for the non-H atoms the difference electron density showed the positions of all H atoms. The positional parameters of the H atoms were included in the refinements with a fixed isotropic displacement factor of 0.03 Å². The absolute structure of the salts was chosen to be in agreement with the known absolute configurations of the cation and anion. This is in accordance with the refined Flack parameter (Flack, 1983) listed in Table 1. Only the data for the (*S*)-mandelate salt was corrected for extinction. The final positional parameters for non-H atoms in the (*S*)- and (*R*)-mandelate salts are listed in Tables 2 and 3, respectively.*

* Lists of atomic coordinates, anisotropic displacement parameters and structure factors have been deposited with the IUCr (Reference: AB0369). Copies may be obtained through The Managing Editor, International Union of Crystallography, 5 Abbey Square, Chester CH1 2HU, England.

Table 3. *Fractional atomic coordinates and equivalent isotropic displacement parameters (Å²) for (R)-mandelate*

$U_{eq} = (1/3)\Sigma_i\Sigma_j U^{ij} a_i^* a_j^* \mathbf{a}_i.\mathbf{a}_j$.

	x	y	z	U_{eq}
O4*A*	0.4411 (2)	0.22863 (4)	0.15799 (10)	0.0236 (2)
N1*A*	0.7113 (2)	0.35760 (4)	0.37576 (13)	0.0268 (3)
N2*A*	0.8311 (2)	0.20179 (4)	0.04372 (12)	0.0211 (3)
C9*A*	0.6785 (3)	0.27997 (5)	0.26234 (13)	0.0201 (3)
C10*A*	0.8700 (3)	0.29134 (5)	0.34190 (14)	0.0209 (3)
C11*A*	1.0524 (3)	0.26607 (5)	0.36922 (14)	0.0232 (3)
C12*A*	1.2322 (3)	0.27922 (6)	0.4445 (2)	0.0281 (3)
C13*A*	1.2394 (3)	0.31850 (6)	0.4976 (2)	0.0289 (4)
C14*A*	1.0656 (3)	0.34326 (5)	0.47463 (15)	0.0277 (3)
C15*A*	0.8778 (3)	0.33075 (5)	0.39679 (14)	0.0237 (3)
C16*A*	0.5388 (3)	0.34555 (5)	0.30125 (15)	0.0263 (3)
C17*A*	0.5149 (3)	0.30733 (5)	0.24239 (14)	0.0236 (3)
C18*A*	0.6576 (2)	0.23905 (5)	0.19738 (13)	0.0190 (3)
C19*A*	0.7714 (2)	0.24291 (4)	0.08804 (13)	0.0190 (3)
C20*A*	0.6454 (3)	0.26658 (5)	−0.02063 (14)	0.0230 (3)
C21*A*	0.6542 (3)	0.24302 (5)	−0.13755 (14)	0.0233 (3)
C22*A*	0.5400 (3)	0.20213 (6)	−0.1336 (2)	0.0276 (3)
C23*A*	0.6450 (3)	0.17779 (5)	−0.0214 (2)	0.0263 (3)
C24*A*	0.9872 (3)	0.20801 (5)	−0.03895 (15)	0.0243 (3)
C25*A*	0.8854 (3)	0.23419 (5)	−0.14937 (15)	0.0245 (3)
C26*A*	1.0085 (3)	0.27244 (6)	−0.1591 (2)	0.0318 (4)
C27*A*	1.0744 (5)	0.28351 (9)	−0.2582 (2)	0.0607 (8)
O4*B*	0.0289 (2)	0.48126 (4)	0.30277 (10)	0.0233 (2)
N1*B*	0.1093 (2)	0.35899 (4)	0.04548 (13)	0.0283 (3)
N2*B*	0.4908 (2)	0.50434 (4)	0.41613 (12)	0.0204 (3)
C9*B*	0.1794 (2)	0.43246 (5)	0.18060 (13)	0.0202 (3)
C10*B*	0.3098 (3)	0.42263 (5)	0.09425 (14)	0.0219 (3)
C11*B*	0.4781 (3)	0.44751 (5)	0.0705 (2)	0.0264 (3)
C12*B*	0.5943 (3)	0.43641 (6)	−0.0156 (2)	0.0335 (4)
C13*B*	0.5507 (3)	0.39971 (7)	−0.0807 (2)	0.0355 (4)
C14*B*	0.3910 (3)	0.37469 (6)	−0.0584 (2)	0.0327 (4)
C15*B*	0.2665 (3)	0.38554 (5)	0.02851 (14)	0.0252 (3)
C16*B*	−0.0066 (3)	0.36954 (5)	0.1259 (2)	0.0275 (3)
C17*B*	0.0216 (3)	0.40577 (5)	0.19479 (14)	0.0235 (3)
C18*B*	0.2129 (2)	0.47126 (5)	0.25676 (13)	0.0199 (3)
C19*B*	0.4006 (2)	0.46453 (5)	0.36328 (13)	0.0200 (3)
C20*B*	0.3461 (3)	0.43816 (5)	0.46719 (14)	0.0223 (3)
C21*B*	0.4198 (2)	0.45965 (5)	0.58882 (14)	0.0225 (3)
C22*B*	0.3003 (3)	0.49997 (5)	0.5890 (2)	0.0269 (3)
C23*B*	0.3430 (3)	0.52675 (5)	0.4835 (2)	0.0237 (3)
C24*B*	0.6975 (2)	0.49602 (5)	0.50102 (15)	0.0233 (3)
C25*B*	0.6593 (2)	0.46938 (5)	0.60854 (14)	0.0224 (3)
C26*B*	0.7959 (3)	0.43158 (6)	0.6219 (2)	0.0276 (3)
C27*B*	0.9434 (3)	0.42382 (7)	0.7185 (2)	0.0386 (4)
O1*A*	0.3819 (2)	0.15654 (4)	0.26121 (12)	0.0309 (3)
O2*A*	0.0433 (2)	0.17436 (4)	0.25104 (10)	0.0249 (2)
O3*A*	0.3388 (2)	0.08458 (4)	0.34974 (13)	0.0306 (3)
C1*A*	0.1958 (2)	0.14980 (5)	0.27276 (13)	0.0209 (3)
C2*A*	0.1489 (3)	0.10713 (5)	0.32049 (14)	0.0224 (3)
C3*A*	−0.0173 (3)	0.08477 (5)	0.22980 (14)	0.0216 (3)
C4*A*	−0.2266 (3)	0.09872 (5)	0.2072 (2)	0.0261 (3)
C5*A*	−0.3791 (3)	0.07947 (6)	0.1213 (2)	0.0311 (4)
C6*A*	−0.3259 (3)	0.04579 (6)	0.0590 (2)	0.0348 (4)
C7*A*	−0.1184 (3)	0.03143 (5)	0.0821 (2)	0.0333 (4)
C8*A*	0.0356 (3)	0.05103 (5)	0.1664 (2)	0.0267 (3)
O1*B*	0.1782 (2)	0.03520 (4)	0.85158 (11)	0.0288 (3)
O2*B*	0.3772 (2)	0.06011 (4)	0.72375 (12)	0.0318 (3)
O3*B*	0.1203 (2)	0.10775 (4)	0.94186 (11)	0.0307 (3)
C1*B*	0.2571 (2)	0.06338 (5)	0.79960 (14)	0.0229 (3)
C2*B*	0.1997 (3)	0.10715 (5)	0.83200 (14)	0.0229 (3)
C3*B*	0.0377 (3)	0.12522 (5)	0.72889 (14)	0.0221 (3)
C4*B*	0.0988 (3)	0.15309 (5)	0.64803 (15)	0.0255 (3)
C5*B*	−0.0501 (3)	0.16901 (6)	0.5533 (2)	0.0326 (4)
C6*B*	−0.2606 (3)	0.15683 (6)	0.5374 (2)	0.0341 (4)
C7*B*	−0.3223 (3)	0.12901 (6)	0.6177 (2)	0.0317 (4)
C8*B*	−0.1739 (3)	0.11337 (5)	0.7131 (2)	0.0263 (3)

Table 4. *Bond lengths (Å), bond angles (°) and torsion angles (°) for the cation in cinchonidinium (S)-mandelate (cd-SM) and cinchonidinium (R)-mandelate (cd-RM)*

	cd-SM	cd-RM *A* molecule	cd-RM *B* molecule
O4—C18	1.416 (2)	1.418 (2)	1.411 (2)
N2—C24	1.503 (2)	1.499 (2)	1.507 (2)
N2—C23	1.506 (2)	1.501 (2)	1.509 (2)
N2—C19	1.510 (2)	1.511 (2)	1.505 (2)
C9—C18	1.524 (2)	1.522 (2)	1.526 (2)
C18—C19	1.545 (2)	1.544 (2)	1.547 (2)
C25—C26	1.504 (2)	1.497 (2)	1.510 (2)
C26—C27	1.311 (3)	1.311 (3)	1.325 (3)
C10—C9—C18	121.53 (13)	121.32 (14)	121.91 (14)
C17—C9—C18	119.61 (13)	120.25 (14)	119.93 (14)
O4—C18—C9	109.87 (11)	110.90 (12)	110.99 (12)
C9—C18—C19	106.47 (10)	107.18 (12)	108.81 (12)
O4—C18—C19	111.64 (11)	110.54 (12)	109.50 (12)
C20—C19—C18	114.49 (12)	114.48 (13)	114.27 (12)
N2—C19—C18	112.17 (10)	111.96 (12)	111.58 (12)
N2—C19—C20	108.13 (10)	108.46 (12)	108.24 (12)
C24—N2—C23	109.51 (11)	109.36 (12)	109.39 (12)
C24—N2—C19	107.93 (10)	108.71 (12)	108.70 (12)
C23—N2—C19	113.84 (11)	113.68 (12)	112.91 (12)
C27—C26—C25	123.9 (2)	123.4 (2)	123.5 (2)
C10—C9—C18—O4	157.88 (12)	160.26 (13)	160.06 (13)
C17—C9—C18—O4	−25.9 (2)	−21.8 (2)	−20.5 (2)
C17—C9—C18—C19	95.1 (2)	98.9 (2)	100.1 (2)
C10—C9—C18—C19	−81.06 (15)	−79.0 (2)	−79.4 (2)
C9—C18—C19—N2	160.05 (12)	159.40 (12)	160.55 (12)
C9—C18—C19—C20	−76.25 (14)	−76.6 (2)	−76.3 (2)
O4—C18—C19—C20	43.66 (14)	44.3 (2)	45.2 (2)
O4—C18—C19—N2	−80.04 (14)	−79.6 (2)	−78.0 (2)
C25—C21—N2—C24	−0.51 (9)	−1.50 (11)	0.90 (10)
C25—C21—N2—C19	116.43 (10)	116.46 (12)	118.91 (11)
C25—C21—N2—C23	−119.57 (10)	−119.99 (12)	−118.25 (12)
C20—C21—N2—C19	−5.22 (10)	−5.21 (11)	−3.04 (10)
C20—C21—N2—C23	118.78 (11)	118.35 (12)	119.80 (12)
C20—C21—N2—C24	−122.16 (11)	−123.16 (13)	−121.06 (12)
C22—C21—N2—C23	−1.42 (10)	−1.49 (11)	−0.40 (11)
C22—C21—N2—C24	117.65 (11)	117.00 (13)	118.75 (12)
C22—C21—N2—C19	−125.41 (11)	−125.05 (12)	−123.24 (12)
C24—C25—C26—C27	125.4 (2)	127.5 (3)	117.0 (2)

3. Results and discussion

3.1. *The conformation of the ions*

The (*R*) salt contains two crystallographically different ion pairs in the asymmetric unit. They are referred to as *A* and *B* in the following. The atomic labelling is adopted from Larsen, Lopez de Diego & Kozma (1993).

3.2. *The cinchonidine cations*

The conformations of the three cations are very similar, as shown by Table 4 which lists bond lengths, bond and torsion angles. The drawing in Fig. 1 illustrates the molecular geometry of the cation in the (*S*)-mandelate salt. The equivalent drawings of cations *A* and *B* in the (*R*) salt are virtually identical. The only significant variations are found in the orientation of the vinyl group with respect to the quinuclidine system, described by the C24—C25—C26—C27 torsion angle. This torsion angle in the *A* ion of the (*R*) salt, 127.6 (3)°, is similar to that found in the (*S*) salt, 125.4 (2)°; in the *B* cation this angle is *ca* 10° smaller. The molecular dimensions of the cation have been compared with those found in the unprotonated base (Oleksyn, 1982) and in the corresponding cinchoninium salts (Larsen, Lopez de Diego & Kozma, 1993). Apart from the variations in the orientation of the vinyl group, the most significant structural changes that occur by the protonization of cinchonidine are the expected elongation of the N2—C bonds from 1.480 (2) to 1.5058 (14) Å and a small decrease in the O4—C18—C19—C20 torsion angle from 48.0 (7) to 44.4 (4)° on average.

The cinchonidinium ion could be expected to be the mirror image of the cinchoninium ion. The bond lengths and angles in the two ions compare very well, but some small variations are observed in the conformation of the ions. The largest differences are observed around the C21—N2 line, as exemplified by the C25—C21—N2—C19 torsion angle which takes values in the range 130.1 (3)–133.73 (14)° in the cinchoninium mandelates and are between 116.43 (10) and 118.91 (11)° in the present study of the cinchonidium salts.

Only the torsion angle that involves the vinyl group shows significant variations in salts of the cinchona alkaloids. The C24—C25—C26—C27 torsion angles in 17 other cinchona alkaloid structures with *R* values less than the 0.10 extracted from the Cambridge Structural

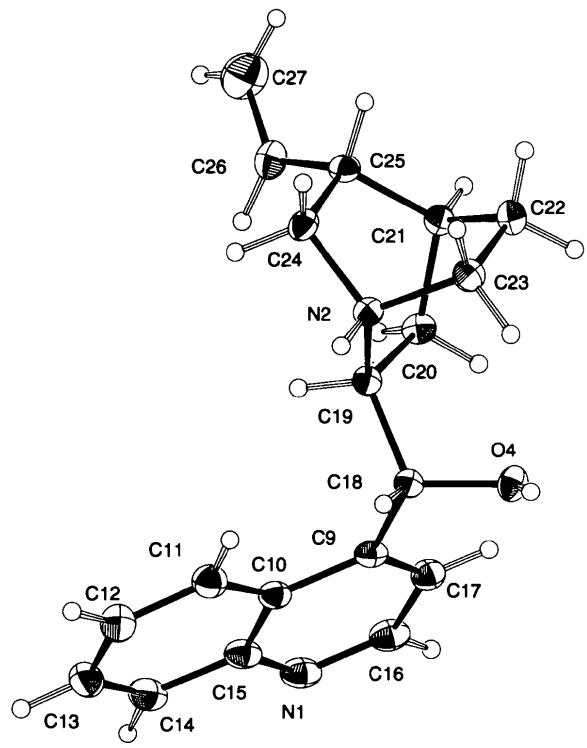

Fig. 1. *ORTEP*II (Johnson, 1976) drawing of the cinchonidium ion in the (*S*)-mandelate salt illustrating the atomic numbering scheme. The thermal ellipsoids enclose 50% probability and the H atoms are drawn as spheres with a fixed radius.

Database (Version 2.3.7; Allen *et al.*, 1979) fall in the range −30 to 180°, with three preferred conformations. The most frequently observed around 120° represents ten structures, with two others being close to 0 and 180°. The differences between the other torsion angles are significantly smaller: less than 25° with the maximum variations around the C9—C18 and C18—C19 bonds. This shows that the two rings constitute a fairly rigid system where only the orientation of the vinyl group varies.

3.3. *The mandelate anions*

In contrast to the rigid cation, the molecular geometry of three mandelate ions exhibit greater variations, as illustrated in Fig. 2 and Table 5. The mandelate ions can be considered as being composed of two planar entities,

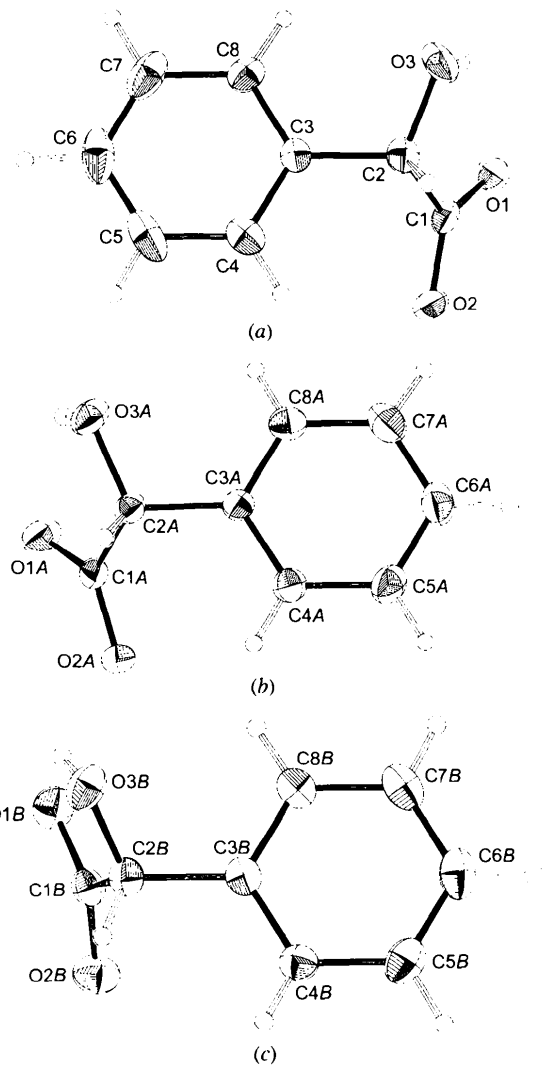

Fig. 2. *ORTEP*II drawings illustrating the atomic labelling of the three mandelate ions found in the two salts. The ions are drawn as the cations in Fig. 1.

Table 5. *Bond lengths (Å), bond angles (°) and torsion angles (°) for the anion in cinchonidinium (S)-mandelate (cd-SM) and cinchonidinium (R)-mandelate (cd-RM)*

	cd-SM	cd-RM *A* molecule	cd-RM *B* molecule
O1—C1	1.249 (2)	1.244 (2)	1.249 (2)
O2—C1	1.259 (2)	1.255 (2)	1.254 (2)
O3—C2	1.416 (2)	1.410 (2)	1.419 (2)
C1—C2	1.541 (2)	1.548 (2)	1.543 (2)
C2—C3	1.516 (2)	1.519 (2)	1.524 (2)
C3—C4	1.394 (2)	1.395 (2)	1.394 (2)
C3—C8	1.390 (2)	1.391 (2)	1.391 (2)
C4—C5	1.390 (2)	1.391 (2)	1.392 (2)
C5—C6	1.375 (3)	1.384 (3)	1.387 (3)
C6—C7	1.383 (4)	1.390 (3)	1.391 (3)
C7—C8	1.395 (3)	1.392 (3)	1.392 (3)
O1—C1—O2	126.06 (14)	126.4 (2)	127.4 (2)
O1—C1—C2	116.35 (14)	116.65 (14)	116.37 (14)
O2—C1—C2	117.6 (2)	116.97 (14)	116.28 (14)
O3—C2—C3	111.69 (12)	111.75 (14)	110.51 (13)
O3—C2—C1	109.83 (14)	109.89 (13)	110.94 (13)
C3—C2—C1	112.25 (11)	111.22 (12)	109.99 (12)
C4—C3—C2	120.28 (14)	119.7 (2)	121.0 (2)
C8—C3—C2	120.6 (2)	121.3 (2)	119.9 (2)
C4—C3—C8	119.1 (2)	119.0 (2)	119.0 (2)
C3—C4—C5	120.5 (2)	120.4 (2)	120.5 (2)
C6—C5—C4	120.2 (2)	120.4 (2)	120.2 (2)
C7—C6—C5	119.9 (2)	119.5 (2)	119.5 (2)
C6—C7—C8	120.4 (2)	120.3 (2)	120.3 (2)
C7—C8—C3	119.9 (2)	120.4 (2)	120.4 (2)
O1—C1—C2—O3	−9.6 (2)	3.9 (2)	18.0 (2)
O1—C1—C2—C3	115.3 (2)	−120.4 (2)	−104.6 (2)
C1—C2—C3—C4	71.0 (2)	−68.5 (2)	−102.4 (2)
O3—C2—C3—C4	−165.10 (13)	168.25 (14)	134.8 (2)

the phenyl group and the carboxylate group. The conformation of the mandelate ion can therefore be described by the two O1—C1—C2—O3 and O3—C2—C3—C4 torsion angles. Intramolecular O3—H3O···O1 hydrogen bonds are formed in the three anions, leading to a five-membered ring. The planarity of the heavy atoms in the ring is described by the O1—C1—C2—O3 torsion angle. The *A* molecule of the (*R*) salt is the most planar with an angle of 3.9 (2)°; in the least planar, the *B* molecule of the (*R*) salt, this torsion angle is 18.0 (2)°. The O3—C2—C3—C4 torsion angle defines the orientation of the phenyl group with respect to the hydrogen-bonded five-membered ring. This angle takes almost the same values in the (*S*) salt and in molecule *A* of the (*R*) salt, 165.10 (13) and 168.25 (14)°, respectively; in the *B* molecule of the (*R*) salt it is *ca* 30° smaller. Since the two anions have opposite absolute configuration, the sign of the torsion angles of the (*S*) salt have been inverted for this comparison. Both the planarity of the O1—C1—C2—O3 moiety and the relative orientation of the phenyl groups are in accordance with the general structural characteristics of the mandelate ion described earlier (Larsen & Lopez de Diego, 1993).

3.4. *The crystal packing*

Inspection of the crystal structures of the two diastereomeric salts revealed that the following interactions

influence the packing: hydrogen bonding, interaction between the planar aromatic groups and the spatial requirement of the vinyl groups. Table 6 contains information on the hydrogen bonds in the two salts. The intramolecular hydrogen bonds between the hydroxy and the carboxylate group have identical O3—H3O···O1 angles in all three mandelate ions, but differ in the O3—O1 distances, the longest distance of 2.640 (2) Å being found in the mandelate ion *B* in the (*R*) salt, where the O3—C2—C1—O1 moiety deviates most from planarity (Table 5).

The carboxylate group of the mandelate ion connects two cations related by translational symmetry along the 6.2777 (6) Å long *b* axis in the (*S*) salt and the 6.410 (3) Å *a* axis in the (*R*) salt. A schematic drawing of the interactions in the infinite chains of alternating cations and anions linked by hydrogen bonds is shown in Fig. 3. In the (*R*)-mandelate salt these hydrogen-bonded chains contain exclusively ions of either type *A* or type *B*.

Inspection of Table 6 reveals that the hydrogen-bond geometry is virtually identical in the two salts. This has led us to conclude that with respect to the hydrogen-bond interactions there are no significant differences between the (*R*)- and (*S*)-mandelate salts of cinchonidine.

Interactions between the planar aromatic ring systems represent another factor that may influence the crystal packing. The stereo pairs in Figs. 4 and 5 reveal a herringbone-like stacking of the quinoline ring systems of cations from two different hydrogen-bonded chains of cations and anions. This particular type of interaction has been observed in several other structures that contain cinchona alkaloids (Oleksyn, Stadnicka & Hodorowicz, 1978; Worsch, Vogtle, Kirfel & Will, 1984; Oleksyn & Serda, 1993). In the (*S*)-mandelate salt (Fig. 4) the cations from the two rows are related by 2_1 symmetry, whereas the two neighbouring rows are made up of independent ions in the (*R*) salt (Fig. 5). The vinyl groups from one row of cations point towards the quinoline systems of the neighbouring row and with the quinuclidine system they form a hydrophobic layer. Both hydrogen-bonding donors point away from these layers, forming hydrogen bonds to an anion layer. The angle between the least-squares planes of quinoline rings in the herringbone arrangement were calculated using the program *PLATON* (Spek, 1990). Almost identical

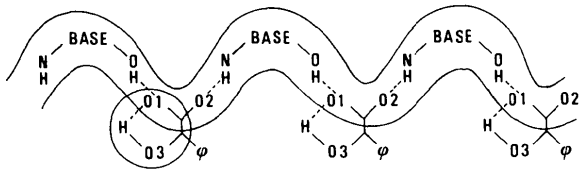

Fig. 3. A schematic drawing of the hydrogen-bonding pattern in the cinchonidinium mandelates. The chain axis corresponds to the *b* axis in the (*S*) salt and to the *a* axis in the (*R*) salt.

Table 6. *Hydrogen-bond interactions in the diastereomeric cinchonidinium mandelates*

	(*S*)-salt	(*R*)-salt *A* molecules	(*R*)-salt *B* molecules
H4O—O1^{i}	1.80 (2)	1.80 (3)	1.72 (3)
H2N—O2^{ii}	1.72 (2)	1.71 (2)	1.75 (2)
H3O—O1	1.99 (2)	2.04 (2)	2.09 (3)
O4—O1^{i}	2.694 (1)	2.691 (2)	2.654 (2)
N2—O2^{ii}	2.647 (2)	2.627 (2)	2.649 (2)
O3—O1	2.592 (2)	2.596 (2)	2.640 (2)
O4—H4O···O1^{i}	169 (2)	173 (2)	174 (2)
N2—H2N···O2^{ii}	168 (2)	162 (2)	163 (2)
O3—H3O···O1	127 (2)	124 (2)	126 (2)

Symmetry codes: for the (*S*) salt: (i) $x, y-1, z$; for the (*R*) salt, molecule *A*: (ii) $1+x, y, z$; for the (*R*) salt, molecule *B*: (i) $-x, \frac{1}{2}+y, 1-z$; (ii) $1-x, \frac{1}{2}+y, 1-z$.

values were found in the two salts, namely 62° in the (*R*)-mandelate and 64° in the (*S*)-mandelate. In the (*S*) salt a similar herringbone stacking is formed of the phenyl groups from anions related by the 2_1 axis, the phenyl–phenyl angle being 45°. In the other diastereomeric salt, which contains anions of opposite chirality, the anions form a head-to-tail arrangement of the phenyl group and the carboxy group of the neighbouring anion. The conformation of the vinyl group is almost identical in the two salts and very similar interactions are observed between this group and the quinoline system.

The two diastereomeric salts differ only with respect to the chirality of the anion and our comparative analysis of their packing has revealed a virtually identical hydrogen-bonding pattern and packing of the cations. The only difference in the packing is found in the arrangements of the phenyl groups.

3.5. *Comparison with the cinchoninium mandelates*

The alkaloids cinchonine and cinchonidine contain four chiral C atoms (C18, C19, C21 and C25). Cinchonine and cinchonidine have opposite chirality at C18 and C19 near the hydrogen-bonding groups. The centres at C21 and C25 have the same absolute configuration in the two alkaloids (Fig. 1). This quasi-enantiomeric relationship between the two alkaloids has sometimes been used to obtain both enantiomers in a resolution (Jacques, Collet & Wilen, 1981). Assuming that salts of cinchonine and cinchonidine display this relationship, equivalence could be expected between the cinchonidine salt of (*S*)-mandelic acid and the (*R*)-mandelate of cinchonine, and similar relations between cinchonidinium (*R*)-mandelate and cinchoninium (*S*)- mandelate. Comparison with the crystal structures of the cinchonine mandelates (Larsen, Lopez de Diego & Kozma, 1993) showed that the two cinchoninium salts display much greater differences, both in the molecular conformations and the crystal packing, than the corresponding cinchonidinium salts. The hydrogen bonds in the cinchoninium (*S*)-mandelate are formed between the same functional groups as the

cinchonidinium mandelate salts, but the hydrogen bond between the hydroxy and carboxy groups links different molecules; two anions connect cations related by a translational symmetry of the 7.0 Å *b* axis. This leads to a herringbone stacking of the quinoline systems from different hydrogen-bonded chains which resembles that found in the cinchonidinium salts. The anions from different chains have their phenyl groups pointing towards each other in an almost coplanar arrangement. The packing of cinchoninium (*R*)-mandelate is completely different both with respect to hydrogen bonds and the stacking of the aromatic ring systems. The schematic drawings shown previously illustrate that cinchonine and the enantiomer of cinchonidine differ only in the relative position of the vinyl group. As the expected quasidiastereomeric salt pairs show completely different crystal packing we can only attribute this difference to the influence of the vinyl group. The effect of the vinyl group can be visualized if one inspects the stereo pairs in Figs. 5 and 6 and imagines the structure with the vinyl groups positioned like cinchonine. This would obviously lead to unfavourable steric interactions, which explains the different packing observed for the cinchonidinium mandelate salts.

3.6. *Optical resolution of mandelic acid by cinchonidine*

This investigation was primarily initiated to attain insight into the structural and physicochemical basis of the resolution of racemic mandelic acid with the cinchona alkaloids. McKenzie (1899) found that although cinchonine gives a slightly better resolution of mandelic acid than cinchonidine, neither are very effective judging from the difference in the solubilities of the diastereomeric salts. He measured the solubilities of the two diastereomeric cinchonidinium mandelates at 292 K in

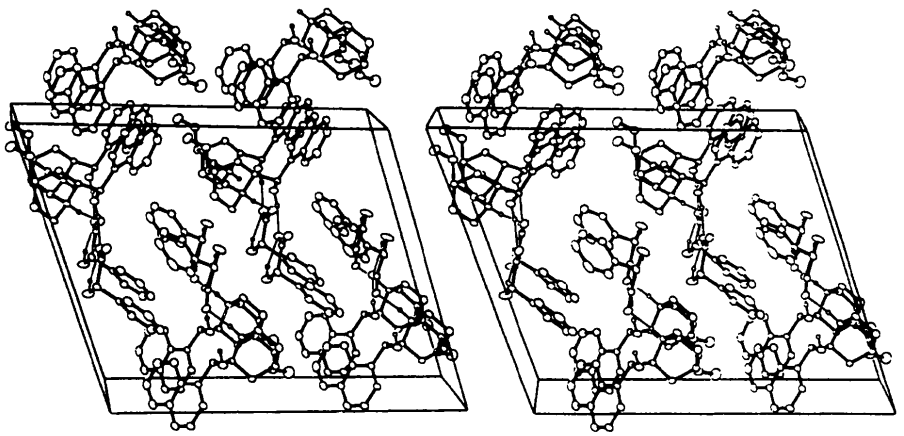

Fig. 4. A stereo pair illustrating the crystal packing in cinchonidinium (*S*)-mandelate. The structure is viewed along the *b* axis, with the *c* axis horizontal. The hydrogen bonds are shown as thin lines.

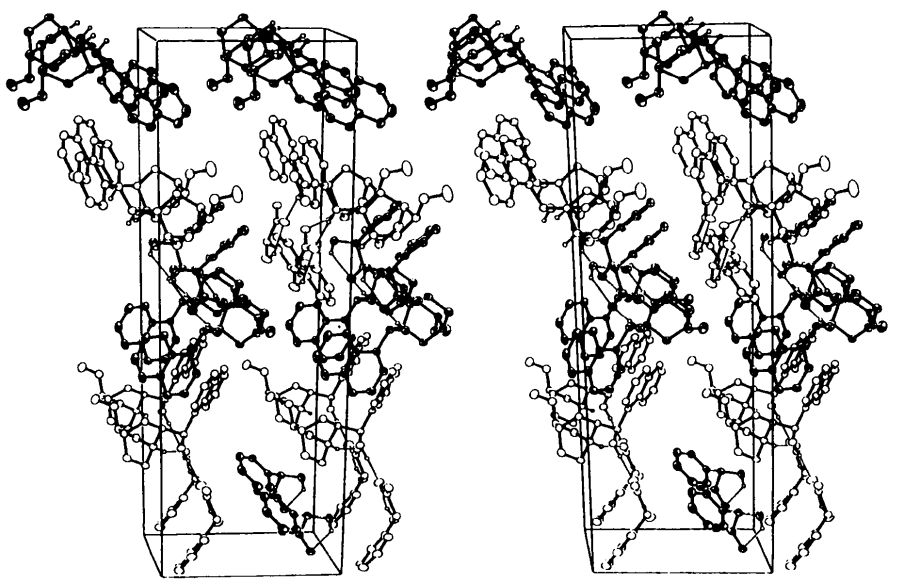

Fig. 5. A stereo pair illustrating the crystal packing in cinchonidinium (*R*)-mandelate. The structure is viewed along **a** with the *c* axis horizontal. The atoms in ion pair labelled *A* are those drawn as shaded footballs. The hydrogen bonds are indicated by the thin lines.

water and ethanol. In agreement with our observation he also found the (*S*)-mandelate salt to be the less soluble salt, but the solubility of the (*R*)-mandelate salt is only slightly higher, 0.89 g of the (*S*) salt and 1.22 g of the (*R*) salt can be dissolved in 100 g of water; the salts are more soluble in ethanol [5.4 and 8.6 g, respectively (McKenzie, 1899)]. In both solvents the solubility of the (*R*) salt is *ca* 1.5 times the solubility of the (*S*) salt. The low solubilities justify the fact that we can assume ideal behaviour of the solutions, *i.e.* the solutions of

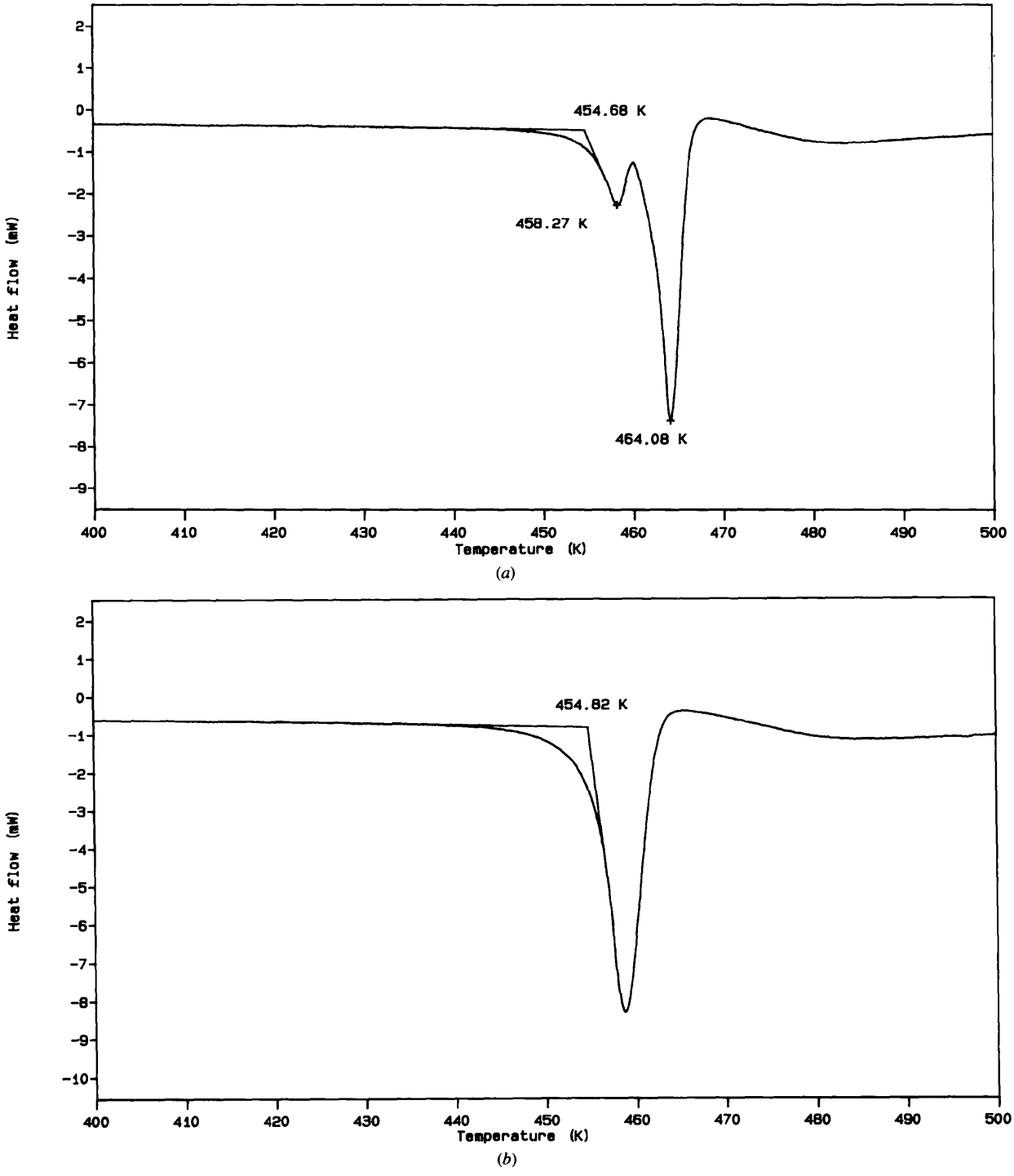

Fig. 6. DSC curves obtained by heating samples of (*a*) cinchonidinium (*R*)-mandelate and (*b*) cinchonidinium (*S*)-mandelate.

the two diastereomeric salts have the same Gibbs free energy. Therefore, the difference in Gibbs free energy at 292 K between the (*R*) and the (*S*) salt can be calculated to be $R292\ln 1.5 \simeq 1\ \mathrm{kJ\ mol^{-1}}$. This difference reflects differences in the enthalpy and entropy of the two salts.

As described above, the two diastereomeric salts have almost identical intermolecular interactions in their crystals. The difference between the structures is found in the conformation of one of the mandelate ions in the (*R*) salt and different interactions between the phenyl groups. These differences can easily account for a difference in free energy of $1\ \mathrm{kJ\ mol^{-1}}$.

3.7. *A solid-state reaction*

The DSC (differential scanning calorimetry) traces for the two salts are shown in Fig. 6. The melting curve for the (*R*) salt has a double peak with minima at 458.3 and 464.1 K. The peak is not caused by impurities, as shown by elementary analysis. Melting was followed visually on a microscope with a hot stage and there seemed to be a partial sublimation with recrystallization just before the actual melting of the sample. The melting of the crystals was accompanied by a change in colour from colourless to reddish brown. The sublimation prior to the melting could explain the double peak in the DSC plot. For the (*S*) salt we record a similar apparent melting point at 454.8 K. When the cooled melts of the salts are heated a second or third time, the melting peaks around 454 K had disappeared and smaller peaks around 310–320 K are observed. These reheating experiments suggest that the melting also involves decomposition and chemical modification.

It has been pointed out that cinchonidine can be converted into its poisonous isomer, cinchonicine, when heated in solution in the presence of a weak organic acid (Biddle, 1912).

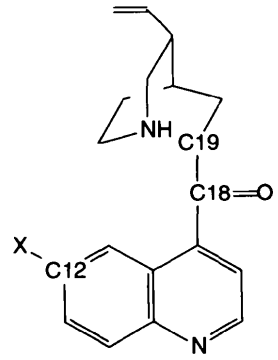

Therefore, it is not unlikely that this reaction can also take place when the salts are heated in the solid state. This assumption is supported by the ^{13}C NMR spectra obtained from the heated salts, which are clearly different from the spectra of the unheated salts. A small peak at approximately 202 p.p.m. is found in the spectra of the heated salts, suggesting the presence of a ketone group in cinchonicine, but not in cinchonidine. In order to assess whether the reaction occurred in the solid state or in the melt, a sample was heated to 438 K (*ca* 16 K below the melting point) and kept at this temperature for 2 h. After cooling the sample it showed a DSC trace that was similar to the traces of the runs of samples that had been heated once to above the melting point, showing that the reaction takes place in the solid state.

To examine the conditions for the reaction to take place in the solid state, DSC measurements were also performed for the free base cinchonidine and the cinchoninium mandelates. The recorded DSC traces for the heating and the reheating experiments of these compounds correspond to normal melting behaviour and indicate that no reaction occurred in these crystals during the melting process.

From this we conclude that reaction in the solid state, as in solution, is catalysed by the presence of the anion. No reaction takes place in crystals of the cinchoninium mandelates, which readily react in solution. This suggests that the packing motif of alternating cations and anions displayed in cinchonidinium salts (Fig. 3) is necessary for the reaction to take place in the solid state.

We thank Dr Peter Andersen for performing the powder diffraction patterns, Dr E. Jonas Pedersen for help with the ^{13}C NMR spectra and Mr Flemming Hansen for assistance in the X-ray diffraction experiments. This research was supported by the Danish Natural Science Research Council. The thermoanalytical equipment was made available through a grant from the Lundbeck Foundation.

References

Allen, F. H., Bellard, S., Brice, M. D., Cartwright, B. A., Doubleday, A., Higgs, H., Hummelink, T., Hummelink-Peters, B. G., Kennard, O., Motherwell, W. D. S., Rodgers, J. R. & Watson, D. G. (1979). *Acta Cryst.* B**35**, 2331–2339.

Biddle, H. C. (1912). *Am. Soc.* **34**, 500–515.

Blessing, R. H. (1987). *Cryst. Rev.* **1**, 3–58.

Enraf–Nonius (1989). *CAD-4 Software*. Version 5.0. Enraf–Nonius, Delft, The Netherlands.

Flack, H. D. (1983). *Acta Cryst.* A**39**, 876–881.

Jacques, J., Collet, A. & Wilen, S. H. (1981). *Enantiomers, Racemates, and Resolutions*, pp. 362–367. Malabar, Florida: Krieger Publishing Company.

Johnson, C. K. (1976). *ORTEP*II. Report ORNL-5138. Oak Ridge National Laboratory, Tennessee, USA.

Larsen, S. & Lopez de Diego, H. (1993). *Acta Cryst.* B**49**, 303–309.

Larsen, S., Lopez de Diego, H. & Kozma, D. (1993). *Acta Cryst.* B**49**, 310–316.

McKenzie, A. (1899). *J. Chem. Soc.* **75**, 964–972.

Oleksyn, B. J. (1982). *Acta Cryst.* B**38**, 1832–1834.

Oleksyn, B. J. & Serda, P. (1993). *Acta Cryst.* B**49**, 530–535.

Oleksyn, B. J., Stadnicka, K. M. & Hodorowicz, S. A. (1978). *Acta Cryst.* B**34**, 811–816.

Pasteur, L. (1853). *C. R. Acad. Sci.* **37**, 110–114.

Sheldrick, G. M. (1990). *Acta Cryst.* A**46**, 467–473.
Sheldrick, G. M. (1993). *SHELXL*93. *Program for Crystal Structure Refinement*. University of Göttingen, Germany.
Spek, A. L. (1990). *Acta Cryst.* A**46**, C34.
Worsch, D., Vogtle, F., Kirfel, A. & Will, G. (1984). *Naturwissenschaften*, **71**, 423–424.